Conception of a Durability Prediction Method for a Metal-Elastomer Machine Mount

Wojciech Sikora[1], Robert Pilch[1*], Maksymilian Smolnik[1]

[1] AGH University of Krakow, Faculty of Mechanical Engineering and Robotics, Department of Machine Design and Maintenance, al. A. Mickiewicza 30, 30-059 Kraków, Poland

* Corresponding author's e-mail: pilch@agh.edu.pl

ABSTRACT

Elastic elements utilised in the support systems of machines are subjects to deterioration processes dependent on the character of their operational loads, work environment and construction. The extent of this change and work time after which it occurs is important information in the maintenance process, necessary for its planning. This paper presents the developed concept of durability prediction method of a four-joint metal-elastomer machine support based on the variation of working temperature of its elastomer elements. Therefore, the solution enables the estimation of significant indexes determining the life cycle of the mount. The developed simulation model is a useful tool for designers, allowing them to estimate the time of the machine mount's correct work. It also helps the operator to schedule the inspections of technical condition (degree of wear) of the machine mount and prepare its replacement operations accordingly. This problem is significant because any failure to an element usually generates higher costs than carrying out a scheduled preventive replacement.

Keywords: durability estimation, elastic mount, random process, designing, maintenance.

INTRODUCTION

Mechanical vibrations are in most cases a side effect of the operation of machines such as e.g. diesel generators, refrigeration units, pumps and fans etc. There are also instances where vibrations are intentionally excited and used to realise specific technological (like bulk material sieving [1]) or transport tasks (vibrating conveyors). Regardless of their character an inevitable phenomenon is the transmission of machine vibrations to its foundation through its supports. These vibrations can have a negative influence on other objects situated nearby, e.g. steel constructions, other machines or technical personnel working in the area. Therefore, a vibration isolation should always be employed to the diminish undesirable effects of these vibrations. In practice, the realisation of vibration isolation requires the selection of proper elastic supports upon which the machine is situated. The relation between force transmitted to the foundation and excitation force applied to the machine is called transmissibility [2] and is described by the following Eq. (1):

$$Tr = \sqrt{\frac{1 + \left(\frac{2\zeta\omega_{ex}}{\omega}\right)^2}{\left[1 - \left(\frac{\omega_{ex}}{\omega}\right)^2\right]^2 + \left(\frac{2\zeta\omega_{ex}}{\omega}\right)^2}} \quad (1)$$

In general, transmissibility depends on the natural angular frequency ω of the system and damping within it. Using an analogy with a simple mass on spring system, the following Eq. (2) for ω can be written:

$$\omega = \sqrt{\frac{k}{m}} \quad (2)$$

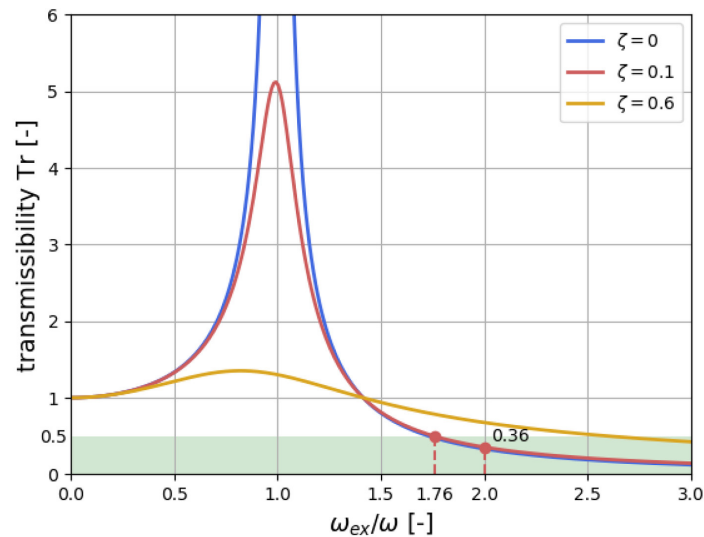Therefore, change in the stiffness of the machine mount will affect vibrations transmissibility.

Fig. 1. Transmissibility for different damping ratio ζ values

In Figure 1, where relation (1) is plotted for selected values of the damping ratio ζ, all the curves intersect at the point where the ratio ω_{ex}/ω is equal to √2. For greater values, the transmissibility *Tr* decreases below 1 and vibration isolation takes place. In the case of machines working with a frequency over their natural frequency, a rapid increase in vibration amplitude in the course of both start-up and run-out [3] must be taken into the account when selecting the machine support. Displacement amplitude limitation is achieved through increasing damping in the system.

Any change in the stiffness of the machine support can have a significant impact on the effectiveness of vibration isolation. In rubber elements stiffness increases with total operation time, which leads decreases in the ratio ω_{ex}/ω.

As can be seen in Fig. 1, the transmissibility factor *Tr* will rise which is undesirable. The results of a numerical simulation aimed at showing the effect of the increasing frequency ω on the transmissibility *Tr* are presented in Figure 2, where the transmissibility is expressed as a relative value, through a reference to its initial value Tr_0. An additional variable a_ω was introduced using Eq. (3) and describes how many times the angular frequency ω increased relatively to its initial value ω_0:

$$\omega = a_\omega \cdot \omega_0 = \sqrt{\frac{a_k \cdot k_0}{m}} \qquad (3)$$

where: $a_k = a_\omega^2$.

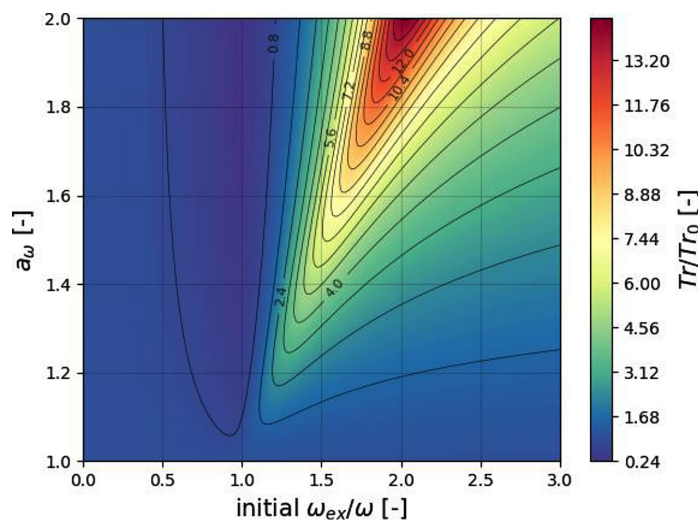This simulation shows that if the machine operates within an isolation range (i.e. $\omega_{ex}/\omega > \sqrt{2}$), a

Fig. 2. Relative transmissibility as a function of the initial ω_{ex}/ω and a_ω for ζ = 0.1

rise in ω causes the same increase in *Tr* and, therefore, worsening of the vibration isolation effect. With a two-fold increase in natural angular frequency, the increase in transmissibility can be even 13-fold which could prevent the further operation of such a machine. For the needs of the analysis performed in this paper it was assumed that the initial ω_{ex}/ω ratio for the analysed technical object would be equal to 2. Therefore an initial transmissibility Tr_0 (Eq. (1)) value will be 0.36 (Fig. 1). Value $\omega_{ex}/\omega = 2$ is arbitrary and in practical application should be based on specific technical requirements for a given system. Thus, from the contour plot in Figure 2 a single curve for $\omega_{ex}/\omega = 2$ was separated and presented in Figure 3 as a 2D plot.

It was assumed that for a given technical object the maximum increase in transmissibility cannot be more than 100%, thus the ratio must satisfy the condition $Tr/Tr_0 \leq 2$. The limit value was marked in Figure 3 and the following values were read: $a_\omega = 1.28$ and $a_k = a_\omega^2 = 1.64$. This means that a two-fold increase in *Tr* corresponds with increasing the system stiffness by 64%.

However, it should be noted that at the same time, depending on the assumed initial absolute values, it is possible for *Tr* to exceed 1 while the condition $Tr/Tr_0 \leq 2$ would still be satisfied.

This would be equal to leaving the effective vibration isolation range. This fact necessitates the checking of not one but two conditions when an allowable value of stiffness change is being selected:
• relative change in transmissibility,
• maximum, absolute value of transmissibility.

The first condition was assumed, as signalled earlier, as $Tr/Tr_0 \leq 2$ which relates to $a_k = 1.64$. The second was selected as $Tr = 0.5$ and marked in Figure 1. The change in transmissibility from the initial value $Tr_0 = 0.36$ to $Tr = 0.5$ results in the ratio $Tr/Tr_0 = 1.39$, which further corresponds, according to Figure 3, with $a_k = 1.29$. Among these two a_k values, the second one is more restrictive, therefore its value, 29%, will be taken as the allowable increase limit in the following calculations. In practical applications, the value of the maximum increase in transmissibility, be it absolute or relative, has to be selected with respect to maintenance requirements for the four-joint elastic mount in a specific application.

Design of a metal-elastomer machine mount and its operation and maintenance processes

There are many different machine supports available on the market. The most popular are helical steel springs, which are versatile and reliable. However, they lack distinct energy dissipating properties, which are important during the run up and coast-down phases of machine operation. Temporary crossing resonance frequency causes undamped system vibration with, theoretically, almost infinite displacement amplitude, which could cause serious damage to the machine itself and its surroundings.

An alternative to helical springs is a metal-elastomer oscillating mount, which consists of four connected Neidhart [4] springs (Fig. 4a and Fig. 4b), making a simple mechanism (Fig. 4c). It allows for greater displacements than simple
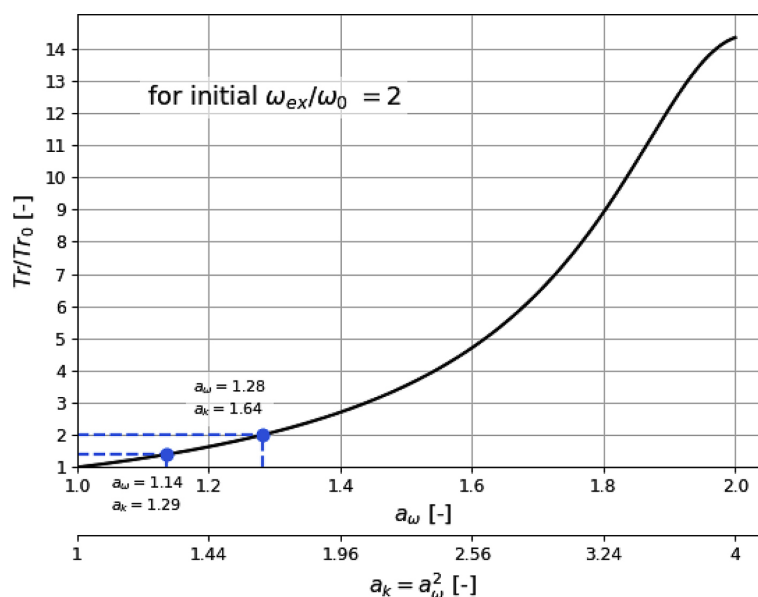

Fig. 3. Slice of the contour plot from Fig. 2 for $\omega_{ex}/\omega = 2$
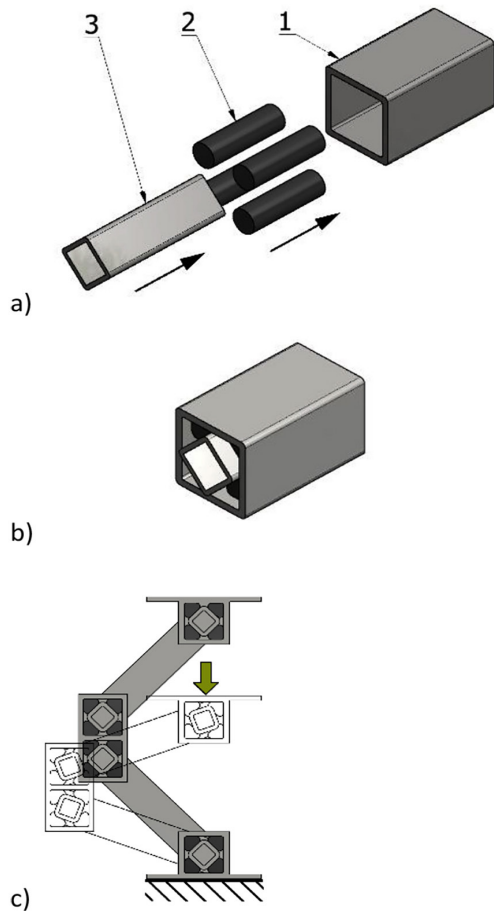
Fig. 4. Design of the Neidhart spring; a) disassembled spring, 1 – square shaft, 2 – cylindrical elastomer inserts, 3 – main body; b) assembled spring; c) four-joint elastic mount

Designing a technical object is not just about determining its structure. It is also necessary to formulate guidelines for its future operation and maintenance which constitute important parts of its life cycle. They should include not only the purpose (scope of application), permissible loads, recommended duty cycle or safety requirements, but also the principles of periodic inspections (their time and scope) and replacement of parts [5, 6]. Thanks to this, maintenance staff have the ability to plan maintenance activities, machine downtime and spare parts inventory. Maintenance guidelines will be subject to verification and possible modifications during the facility operation and maintenance process. To safely start the operation process, however, one needs to have some initial (basic) operating recommendations that relate to changes in the technical condition of the machine forecast by the designer. The designers therefore need forecasting tools that allow them to estimate the future durability and reliability of the designed object.

The aim of this work is to present a procedure which can be utilised for the assessment of reliability and durability of a metal-elastomer mount (Fig. 4c) at its design stage, which is of great practical importance [7]. Reliability in this case will be interpreted as the probability of ensuring the acceptable level of stiffness for exemplary mechanical systems within the set time horizon and operation conditions.

Elastomer ageing

Elastomer ageing is actually modification of its chemical structure over time, which appears as a noticeable change in its mechanical properties. This process occurs from the moment the elastomer is cured and the final product is obtained. If elastomer elements are stored properly, the ageing process is not a serious problem, however, extended periods of storage should also be avoided too [8]. Ageing becomes significant when the elastomer element goes into service and operates e.g. as an o-ring seal or elastic spring in a mechanical system. Then, ageing is influenced by environmental conditions (i.e. humidity, contact with industrial fluids, ambient temperature, radiation [9, 10]) and variable mechanical loading (i.e. force, pressure, deformations).

It is difficult to clearly describe mechanisms responsible for elastomer ageing. In the literature [11, 12], the following are mentioned: loss

rubber springs and has satisfactory damping properties. Each spring consists of two metal square hollow sections between which four elastomer cylinders are squeezed during its assembly. Springs are in fact torsional, but thanks to connecting them using metal bars (Fig. 4c), the whole mount becomes a mechanism which can deform vertically similarly to helical spring. Additionally, it can also work effectively in the horizontal direction.

The general technical condition of machine supports deteriorates with time during their operation. In the case of a steel helical spring, it may be material fatigue that leads to its abrupt failure. For metal-elastomer mounts however, a change in its mechanical properties due to elastomer ageing is more significant. Consequently, the stiffness of a mount changes which further involves modification of the whole system dynamics, including vibration transmissibility. For this reason, in order to prevent such adverse changes, it is necessary to conduct proper technical maintenance in the process of mount operation.

of plasticisers, oxidation, crosslink creation and chain scissions. Which of them actually plays a role and to what extent depends on many factors. The most important is the chemical composition of the elastomer compound. It can cause interesting situations, like one described in [12]. Two different chemical degradation processes were counterbalancing each other during the experiment. Therefore, one of the significant elastomer properties changed only slightly after ageing. However, identifying actual relations between chemical components and the degradation process of elastomers is a difficult task requiring the use of more sophisticated methods, e.g. FTIR spectroscopy [13].

The prediction of changes in properties during the operation of products made from elastomers is a topic often covered in publications [14-16]. Knowledge about the variability of a material's properties is essential for predicting its durability and making decisions on its replacement [17]. It can be utilised both at the product design stage and later during operation. Natural ageing processes usually take several, up to even dozens of years [18]. Monitoring the elastomer condition for such a long time is troublesome. Therefore, instances where data from a long time span observation is available are rare. An answer to this issue are accelerated-ageing tests. The general idea behind tests is to place elastomer specimens inside an oven, where constant a temperature is maintained. The details are given in the standard [19]. Long-term exposure to elevated temperatures (i.e. higher than room temperature) intensifies elastomer ageing, thus it is often used as a way to predict material condition after extended periods of operation. Depending on the aim of accelerated-ageing tests, specific material properties are measured after each test. Usually, the mechanical properties are of the main interest, thus e.g. uniaxial tensile testing is performed with recording of the stress and strain relation. In many cases the Arrhenius model is used to describe changes in material properties due to time and temperature influence. Works can be found in the literature [20] where authors successfully employed the said model to describe the ageing of various elastomer materials. It should be mentioned that the Arrhenius relation is based on the assumption that elevated temperature influences only the intensity of ageing processes, while the character and type of deterioration mechanisms remain the same as at room temperature [21].

Research results regarding the variability of elastomer mechanical parameters during accelerated ageing can be found in [22]. In the mentioned work a rubber mixture based on chloroprene (CR) was described as Mooney-Rivlin material [23], therefore the investigated parameters were C_{01} and C_{10} utilised in constitutive equations for this material type. The Arrhenius equations, Eq. (4) and Eq. (5), determined in the cited paper for both parameters were the following:

$$C_{10}(t,T) = x_{10} \cdot \exp\left[\begin{array}{c} A_{10} \cdot t \cdot \\ \cdot \exp\left(-\dfrac{E_{a,10}}{RT}\right) \end{array}\right] \quad (4)$$

where: x_{10} = 0.192 MPa,
A_{10} = 6.01·10^7 hr^{-1},
$E_{a,10}$ = 74.9 kJ/mol,
R = 8.314 J·K^{-1}·mol^{-1}.

$$C_{01}(t,T) = x_{01} \cdot \exp\left[\begin{array}{c} A_{01} \cdot t \cdot \\ \cdot \exp\left(-\dfrac{E_{a,01}}{RT}\right) \end{array}\right] \quad (5)$$

where: x_{01} = 0.399 MPa,
A_{01} = 2.26·10^7 hr^{-1},
$E_{a,01}$ = 71.8 kJ/mol.

Equation (4) and (5) with their coefficients were further used to estimate ageing processes (cf. [9, 24]) in rubber cylinders responsible for the elastic properties of four-joint metal-elastomer mounts which is the subject of the next section.

Estimating durability of a metal-elastomer machine mount

Elastic elements that undergo cycles of loading due to internal damping dissipate a part of the energy used to deform them. In the case of rubber elements, the amount of energy lost due to this phenomenon can be from a few to several dozen percent, depending on the application and their purpose. Temperature is an important factor that decides on the intensification of ageing processes. In the works [25-27], one can find results showing that the temperature of rubber elements in stable working conditions can reach up to 90 °C. Therefore, in this analysis it was assumed that the temperature of the rubber element and time of the exposure to the specific temperature will be used to describe the operation process of a four-joint metal-elastomer machine support. The model consists of the consecutive stages described in the following subsections:

- designation of elastomer temperature variation history in a given time range,
- determination of changes in material parameter values over time,
- calculation of the mount stiffness for given material parameters after ageing,
- basing on the partial cumulative distribution function (CDF), determining the time range during which the mount will operate properly.

Figure 5 shows a diagram of the procedure for estimating the design durability of a machine mount and its possible verification in operational tests. Operational durability is determined on the basis of observed changes in diagnostic signals of physical objects during their actual operation.

Design durability can be estimated using method presented in this study.

The obtained results and their comparison give the opportunity to evaluate the adopted design method as well as the developed method of estimating design durability. They also provide information on the directions of improvement for the designed shock absorber construction solution. The study presents a method for estimating (a priori) the design durability of a selected shock absorber.

Simulation of temperature variation over time

In the developed model the temperature of the rubber element within the metal-elastomer mount is the primary signal describing the actual
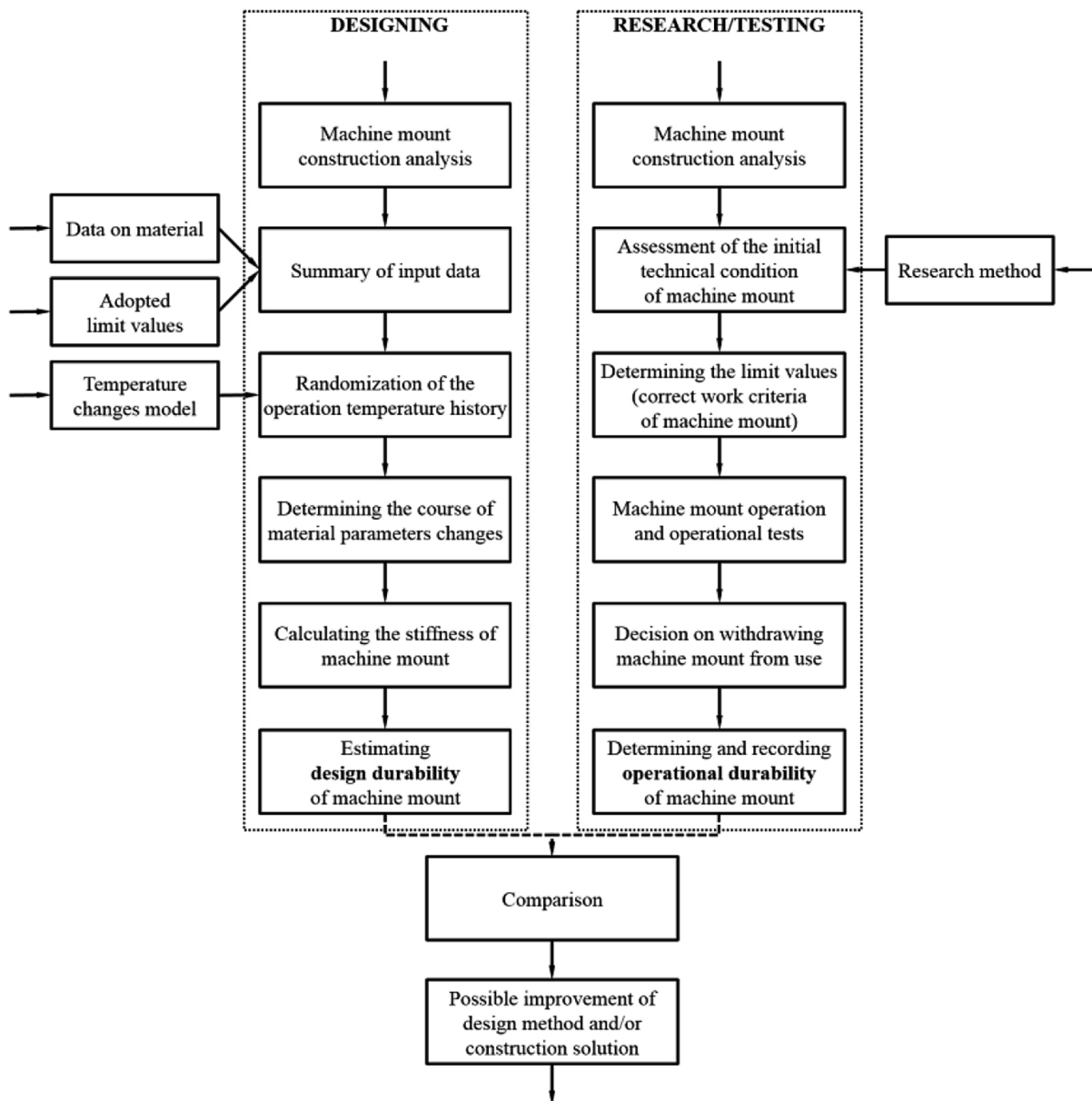

Fig. 5. Diagram of the procedure for estimating the design and operational durability of a machine mount

working conditions of the mount and is dependent directly on the mechanical loads it is subject to. As an external excitation changes, causing a variation in load amplitude, the same will happen with rubber cylinder deformations. It will influence the amount of dispersed energy due to damping and also the temperature value itself. Actual machine loads are variable over time. The described variability is the main source of randomness that influences the probability distribution of a four-joint metal-elastomer mount's reliability. Therefore, the temperature history over time is a random process.

In the beginning, a time range for the simulation t_{total} has to be defined. It is expressed in hours and concerns only working periods of the machine mount. Periods when the machine does not operate are omitted, because then the temperature of rubber elements falls to environment temperature, which is assumed to be ca. 22 °C. For such a temperature level, ageing processes estimated through the Arrhenius model (Eq. (4) and Eq. (5)) would cause a negligible change in material properties.

Next, the time range t_{total} has to be discretised into identical periods of length Δt, which is also one of the model input parameters. For each of the $n = t_{total}/\Delta t$ periods a value of the rubber cylinder is drawn according to selected random distribution. It was assumed that these periods are independent of each other and temperature remains constant for their duration. The distribution used in this simulation is a normal distribution described by the parameters μ and σ that are constant for each period within the time range t_{total}. Normal distribution best describes the random character of temperature variations, which can take place in practice. It is possible to modify the model by choosing different kinds of distribution.

Figure 6 is presents an example of how temperature variation, obtained according to the earlier described method, can look for $t_{total} = 20\ 000$ hr and $\Delta t = 8$ hr. The parameters of normal distribution were the following: $\mu = 40$ °C and $\sigma = 10$ °C.

In summary, steps required to obtain temperature variation in time are following:
- designation of the total time range t_{total},
- discretization of the time range into periods of Δt,
- generation of random temperatures T using inverse CDF method for each of periods.

Single realisation of the temperature variation process is insufficient for investigating the randomness of the whole process.

Therefore, it is necessary to generate a larger number of such curves, which, as with the general idea, is similar to the Monte-Carlo method [28, 29]. The number of realisations of the temperature random variation process is marked in the model as N.

Translation of temperature variation to material parameters

In the second stage of the model the temperature history is translated to the variation of the material parameters C_{10} and C_{01}. Based on
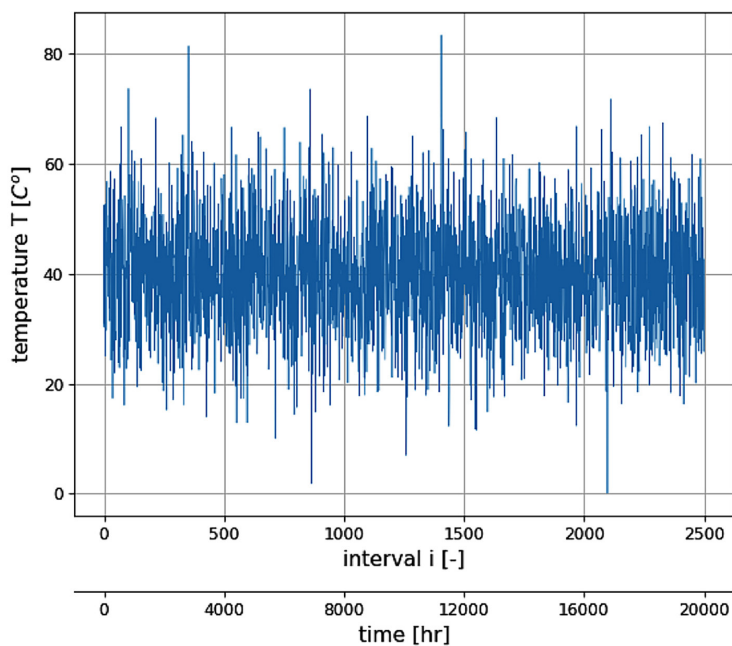

Fig. 6. Example of a single realisation of the temperature random variation process for a given time range
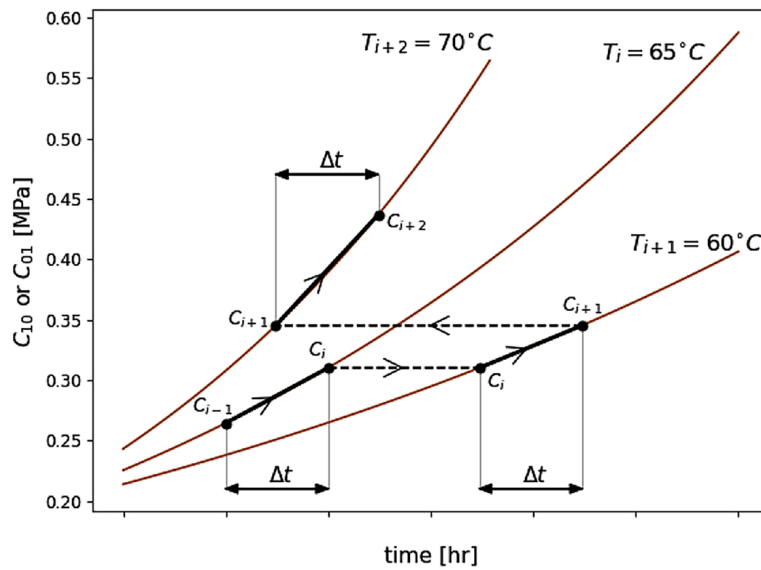
Fig. 7. Method of calculating new values of C_{10} and C_{01} parameters for consecutive time periods based on Arrhenius equations and selected temperatures
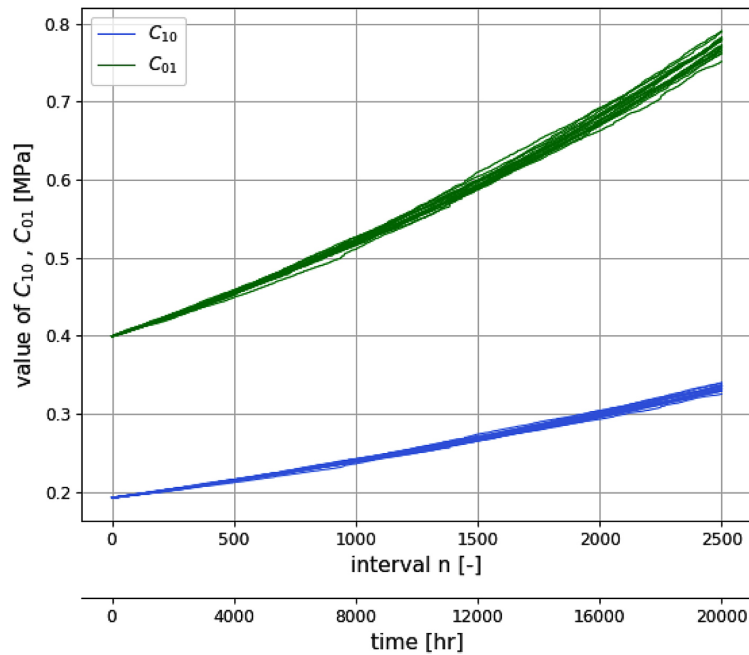

Fig. 8. Translated parameter variation over time for $N = 20$

Eq. (4) and Eq. (5) values of both parameters are estimated for each of the time periods numbered by $i = 1, 2, 3, ..., n$. The obtained values correspond with the state of material at the end of each period, after the time Δt has passed. At the start, when time $t = 0$, initial values of C_{10} and C_{01} are equal to, respectively, x_{10} and x_{01}. After time Δt, when the rubber element is exposed to the temperature T_i, the material properties change. New values of C_{10} and C_{01} are calculated based on the Arrhenius model. Because of the nonlinearity of relationships (Eq. (4) and Eq. (5)) it is necessary

to track the values of C_{10} and C_{01} at the end of each consecutive period, which will become boundary conditions in the next period. The method for calculating the Mooney-Rivlin material parameters is presented in Figure 7 for three consecutive example periods Δt where temperature changed to, respectively, 65 °C, 60 °C and 70 °C.

Translation of each of the N curves $T(t)$ (like in Fig. 6) results in a single pair of curves $C_{10}(t)$ and $C_{01}(t)$. The example set of $N = 20$ such pairs is shown in Figure 8. The data set obtained in that manner is a base to carry out further analysis.

Method of determining CDF based on partial distributions

The data set containing N realisations of elastomer temperature random variation, translated to a variation of material parameters C_{10} and C_{01}, allows determination of the partial probability distribution for each time period $i = 1, 2, 3, ..., n$. In this way, the occurrence probability for each pair of C_{10} and C_{01} can be estimated for a given Δt. However, it is necessary to maintain the connection within each pair and not lose it during analysis, as for each obtained value of C_{10} from Eq. (4) one value of C_{01} from Eq. (5) is also calculated. To achieve this, for each period i a similar 3D histogram is made, like the one presented in Figure 9. Values of C_{10} and C_{01} are divided into 10 bins, which gives a total of 100 bins within which occurrences of specific values are counted. For example, in Figure 9, the probability that C_{10} and C_{01} would have values from the range with a middle value equal to $C_{10} = 0.41029$ MPa and $C_{01} = 0.9629$ MPa is 0.256. In the given example from among 100 bins only 23 are described by a nonzero probability, which is directly related to the standard deviation σ in the assumed normal distribution. The bigger the deviation, the more bins in the histogram are described by a non-zero probability.

After obtaining the distribution of the material parameters (Fig. 9) the next step is determining how they influence the stiffness of the four-joint metal-elastomer mount. The mount response

during vertical compression is acquired through the finite element method (FEM) calculation in the ANSYS environment, while the middle values from bins in a given histogram (similar to the one in Figure 9) were adopted as the values of parameters C_{10} and C_{01}. Mechanical boundary conditions were following: bottom joint was fixed to the ground (Fig. 4c) and both top and bottom joint remained aligned during vertical deflection. More information about FEM modelling of Neidhart springs can be found in [30]. By referencing single joint calculation results to the whole four-joint mount kinematics it is possible to obtain its compression curve and further determine its local stiffness at the working point. For the histogram from Figure 9, a total of 23 FEM calculations have to be performed and the probability for each obtained mount stiffness would be equal to proper values from Figure 9. An example of a partial CDF of mount stiffness for a single time period is presented in Figure 10.

Single dots represent results from bins with nonzero probability in a histogram. Based on these discrete points it is possible to calculate the partial empirical CDF for a given period Δt. Usually, because of the assumed number of bins and number N of temperature random variation process realisations, the course of the curve resembles a broken line. This makes it difficult to properly read the value of CDF for a given stiffness. It is a typical outcome for simulations of random processes that can be limited by increasing the
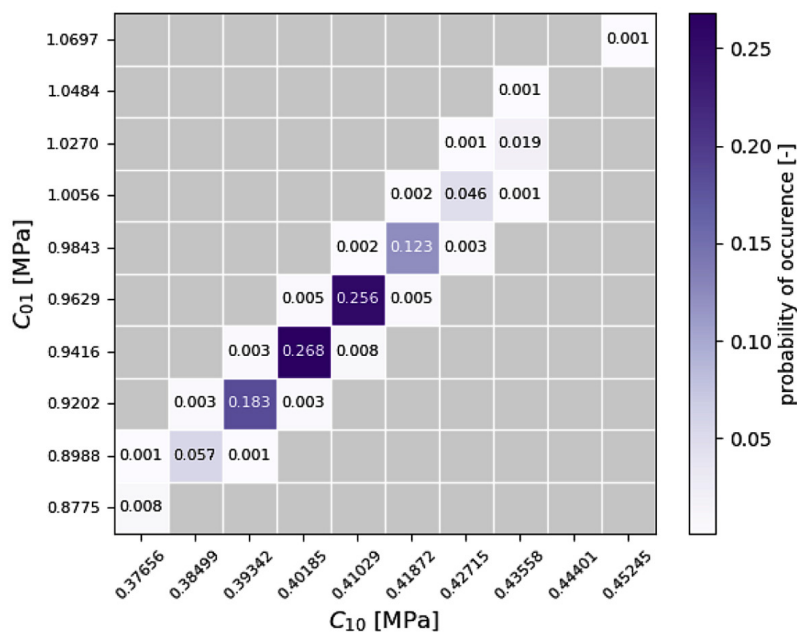
Fig. 9. Example 3D histogram of occurrence probability for the parameter pair C_{10} and C_{01}
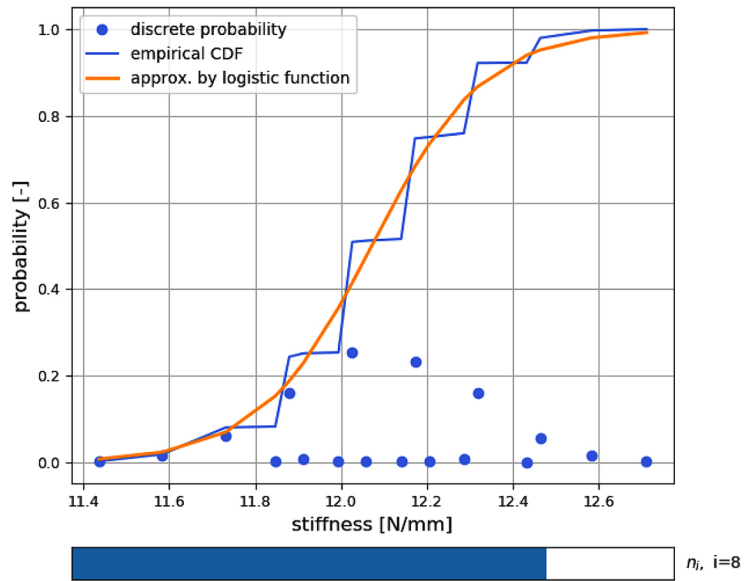
Fig. 10. Example of a partial CDF for a single time period based on a histogram
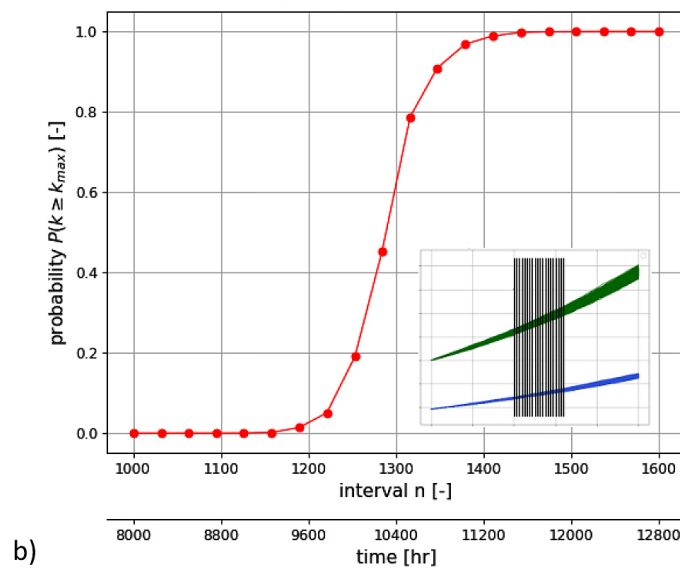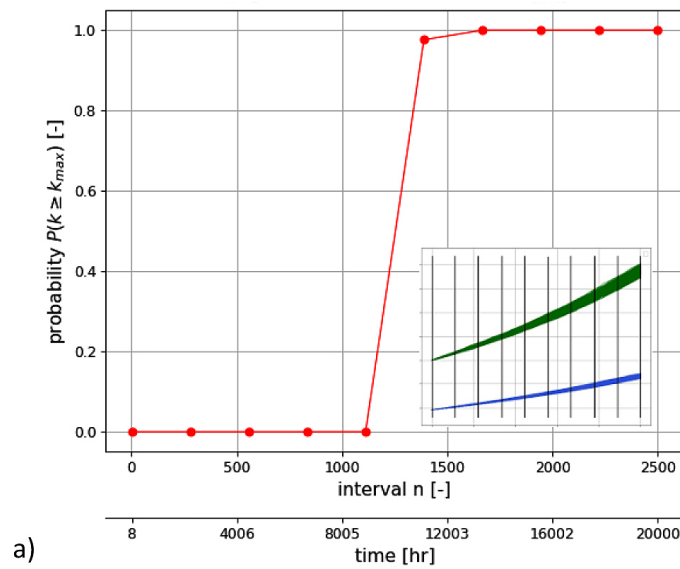

Fig. 11. Consecutive simulation iterations for calculating the final CDF; a) 1st iteration; and b) 2nd iteration

number of repetitions N and bins in histograms. This, however, increases the computational time of the whole simulation. Despite the unfavourable shape, the received empirical CDF reflects well the general trend of probability change and therefore it was proposed to approximate it with a logistic function – see Eq. (6) [31-34]:

$$f(t) = \frac{1}{1 + exp[-b_1 \cdot (t - b_0)]} \tag{6}$$

where: b_0, b_1 – coefficients determined during approximation.

Having a continuous empirical partial CDF, it is possible to find the probability $P(k \geq k_{crit})$ where k_{crit} is the maximum allowable value of the mount stiffness. In this case it was assumed, corresponding with Fig. 3, as $k_{crit} = 1.29k_0$. The probability values read for consecutive time periods Δt would allow the final CDF $P(k(t) \geq k_{crit}) = g(t)$ to be obtained, which is a function of time and delivers information about the maximum allowable total operation time of the four-joint mount. Because of the fact that, for preparing a single partial CDF, it is necessary to perform from a few to several dozen FEM simulations (it depends on the normal distribution deviation which influences the number of non-zero bins in 3D histograms), assembling the final CDF is carried out iteratively and for only a selected number of time periods. For example, Fig. 11a shows the first iteration of the simulation, with the aim to find the time for which the CDF value changes instantly. The second iteration in Fig. 11b allows verification of the earlier result and the final form of CDF to be obtained. The first iteration was conducted for 10 partial CDFs and the second one for 20, which allowed a more accurate result to be obtained.

DISCUSSION

The results obtained and illustrated in Fig. 11 allow determination of the probability of the event that after a specified time of operation the analysed machine mount exceeds the adopted stiffness limit value. It should be remembered that the obtained results are conditioned by the adopted ageing model of the elastomer, its mechanical parameters and the probability distribution of changes in the mount operating temperature. Changing such data will lead to other results. This provides the option to estimate the durability for various distributions of elastomer operating temperature changes using the developed computational model, and thus to forecast the durability of machine mounts operating in different temperature conditions and various adopted stiffness limits.

It should also be noted that the logistic distribution adopted for the description of machine mount stiffness can be replaced by classic probability distributions often used in reliability engineering (normal, Weibull, Gamma), with appropriate parameters matched in goodness-of-fit tests (cf. [35]). In some cases, they will probably more accurately reflect the nature of the changes shown by the obtained histogram. However, the main purpose of this paper is to present the developed calculation method and model, and not to discuss matching the probability distribution to the partial calculation results, which was not the most important element here.

The use of the developed model for estimating the durability of a machine mount in practical applications also requires the determination of the ω_{ex}/ω ratio at the beginning. It determines the nominal level of transmissibility and, at the acceptable level of deterioration, determines the extent of the allowable increase in elastomer stiffness occurring as a result of its ageing over time. Therefore, assuming the value of the ω_{ex}/ω ratio will affect the estimated durability of the machine mount.

CONCLUSIONS

In the process of operation and maintenance of technical objects, there is currently a goal maximise their use (i.e. to replace their parts just before reaching the limit state or before their failure) while minimising the probability of unforeseen failure (which may cause a safety risk, losses due to damage to other elements and additional costs because of longer machine downtime) – cf. [36]. To achieve this goal, it is necessary to carry out inspections and, if possible, to check the technical condition on a continuous basis. This problem is much simpler if the designer and the operator already know before the start of the operation process about the estimated time of durability and the time of correct work of the element under given conditions.

The developed simulation model for estimating the durability of a metal-elastomer machine mount is a useful tool for designers. When using it, it is possible to estimate the time in which

the machine mount will work correctly under specified conditions with a given probability. This knowledge also allows the future operator to plan the time to check the technical condition (degree of wear) of the machine mount and plan and prepare its replacement operations accordingly. This problem is significant because any failure to an element usually generates higher costs (resulting from unplanned downtime or possible damage to other elements) than carrying out a scheduled preventive replacement at a pre-determined time. Therefore, knowing how long the machine mount can work under given conditions is desirable and also allows replacements to be scheduled shortly before it reaches its estimated limit state, thus maximising the utilisation of its durability resource.

With the help of the developed method, it is also possible to make an attempt to construct the machine mount so that in the given (adopted) operating conditions it will work for the required time. This reduces the need to conduct laboratory or operational tests of manufactured objects, allowing an initial picture of the relationship between the decisions of the designer and the expected future course of the operation process to be obtained at a low cost.

Acknowledgements

Nomenclatures

Tr – transmissibility [−],
Tr_0 – initial transmissibility [−],
ω – undamped angular natural frequency of the system [s^{-1}],
ω_0 – initial angular frequency of the system (support) [s^{-1}],
ω_{ex} – angular frequency of an external excitation [s^{-1}],
ζ – damping ratio [−],
k – local stiffness of the system [N/mm],
k_0 – initial stiffness of the system (support) [N/mm],
k_{crit} – a maximum allowable value of the mount stiffness [N/mm],
m – supported mass [kg],
a_ω – change coefficient of an angular frequency [−],
a_k – change coefficient of a stiffness [−],

C_{10}, C_{01} – material constants [MPa],
T [K] – temperature,
t – time [hr],
x_{10}, x_{01} – initial values of C_{10}, C_{01} [MPa],
A_{10}, A_{01} – pre-exponential factor in Arrhenius equation [hr^{-1}],
$E_{a,10}, E_{a,01}$ – activation energy [kJ/mol],
R – gas constant [$J \cdot K^{-1} \cdot mol^{-1}$],
t_{total} – a time range for the simulation [hr],
Δt – a time period duration [hr],
μ – mean of a normal probability distribution [°C],
σ – standard deviation of a normal probability distribution [°C],
N – number of realisations of the temperature random variation process [−].

REFERENCES

1. Yan H., Li Y., Yuan F., Peng F., Yang X., Hou X. Analysis of the Screening Accuracy of a Linear Vibrating Screen with a Multi-layer Screen Mesh. Strojniski Vestnik/Journal of Mechanical Engineering 2020; 66: 289–299, DOI: 10.5545/sv-jme.2019.6523.

2. Harris C., Piersol A. Harris' Shock and Vibration Handbook, McGraw-Hill handbooks. McGraw-Hill: 2002.

3. Cieplok G. Verification of the nomogram for amplitude determination of resonance vibrations in the run-down phase of a vibratory machine. Journal of Theoretical and Applied Mechanics 2009; 47: 295–306, https://www.researchgate.net/publication/265919414.

4. Neidhart H.J. Elastic joints. US Patent 2,712,742, 1955.

5. Młynarski S., Pilch R., Smolnik M., Szybka J., Wiązania G. A model of an adaptive strategy of preventive maintenance of complex technical objects. Eksploatacja i Niezawodnosc – Maintenance and Reliability 2020; 22(1): 35–41, DOI:10.17531/ein.2020.1.5.

6. Pilch R. A method for obtaining the required system reliability level by applying preventive maintenance. Simulation: Transactions of the Society for Modeling and Simulation International 2015; 91: 615–624, DOI:10.1177/2F0037549715592274.

7. Kuraś Ł.M., Smolnik M. Modernisation of LEMACH 6 Design-Research Method as a Reliability Engineering Tool. Journal of KONBiN 2020; 50(2): 145–164, DOI:10.2478/jok-2020-0032.

8. Guo F., Jia X., Huang L., Salant R.F., Wang Y. The effect of aging during storage on the performance of a radial lip seal. Polymer Degradation and Stability 2013; 98: 2193–2200.

9. Pham H. (Ed.) Handbook of Reliability Engineering. London, Springer-Verlag: 2003.

10. Pourmand P., Hedenqvist M., Furó I., Gedde U. Radiochemical ageing of highly filled EPDM seals as revealed by accelerated ageing and ageing in-service for 21 years. Polymer Degradation and Stability

2017; 144: 473–484.

11. Gac P.L., Saux V.L., Paris M., Marco Y. Ageing mechanism and mechanical degradation behaviour of polychloroprene rubber in a marine environment: Comparison of accelerated ageing and long term exposure. Polymer Degradation and Stability 2012; 97: 288–296.

12. Kömmling A., Jaunich M., Wolff D. Effects of heterogeneous aging in compressed HNBR and EPDM o-ring seals. Polymer Degradation and Stability 2016; 126: 39–46, DOI:10.1016/j.polymdegradstab.2016.01.012.

13. Celina M., Wise J., Ottesen D., Gillen K., Clough R. Correlation of chemical and mechanical property changes during oxidative degradation of neoprene. Polymer Degradation and Stability 2000; 68: 171–184.

14. Chou H.W., Huang J.S. Effects of cyclic compression and thermal aging on dynamic properties of neoprene rubber bearings. Journal of Applied Polymer Science 2007; 107: 1635–1641.

15. Saux V.L., Gac P.L., Marco Y., Calloch S. Limits in the validity of Arrhenius predictions for field ageing of a silica filled polychloroprene in a marine environment. Polymer Degradation and Stability 2014; 99: 254–261, DOI:10.1016/j.polymdegradstab.2013.10.027.

16. Woo C.S., Park H.S. Useful lifetime prediction of rubber component. Engineering Failure Analysis 2011; 18: 1645–1651, DOI:10.1016/j.engfailanal.2011.01.003.

17. Hassine M.B., Naït-Abdelaziz M., Zaïri F., Colin X., Tourcher C., Marque G. Time to failure prediction in rubber components subjected to thermal ageing: A combined approach based upon the intrinsic defect concept and the fracture mechanics. Mechanics of Materials 2014; 79: 15–24.

18. Oldfield D., Symes T. Long term natural ageing of silicone elastomers. Polymer Testing 1996; 15: 115–128.

19. ISO 188. Rubber, vulcanized or thermoplastic – accelerated ageing and heat resistance tests. Geneva, International Organization for Standardization: 2011.

20. Gac P.Y.L., Celina M., Roux G., Verdu J., Davies P., Fayolle B. Predictive ageing of elastomers: Oxidation driven modulus changes for polychloroprene. Polymer Degradation and Stability 2016; 130: 348–355, DOI:10.1016/j.polymdegradstab.2016.06.014.

21. Davies P., Evrard G. Accelerated ageing of polyurethanes for marine applications. Polymer Degradation and Stability 2007; 92: 1455–1464.

22. Ha-Anh T., Vu-Khanh T. Prediction of mechanical properties of polychloroprene during thermo-oxidative aging. Polymer Testing 2005; 24: 775–780.

23. Bower A.F. Applied Mechanics of Solid. CRC Press: 2009.

24. Tobias P.A., Trindade D.C. Applied Reliability. Third Edition. Boca Raton, CRC Press Taylor and Francis Group: 2012.

25. Banic M., Stamenkovic D., Miltenovic V., Milosevic M., Miltenovic A., Djekic P., Rackov M. Prediction of heat generation in rubber or rubber-metal springs. Thermal Science 2012; 16: 527–539, DOI:10.2298/TSCI120503189B.

26. Luo R.K., Wu W.X., Mortel W.J. A method to predict the heat generation in a rubberspring used in the railway industry. Proceedings of the Institution of Mechanical Engineers, Part F: Journal of Rail and Rapid Transit 2005; 219: 239–244.

27. Luukkonen A., Sarlin E., Villman V., Hoikkanen M., Vippola M., Kallio M., Vuorinen J., Lepistö T. Heat generation in dynamic loading of hybrid rubber-steel composite structure. ICCM17 Edinburgh, 17th International Conference on Composite Materials, 27-31 July 2009, Edinburgh, UK. 2009.

28. Faulin J., Juan Perez A.A., Martorell Alsina S.S., Ramirez-Marquez J.E. (Eds.) Simulation Methods for Reliability and Availability of Complex Systems. London, New York, Springer: 2010.

29. Johnson P.E. Monte Carlo Analysis in Academic Research. In: Little TD. (ed.) The Oxford Handbook of Quantitative Methods in Psychology, 1. Oxford, Oxford University Press: 2013: 454–479.

30. Sikora W., Michalczyk K., Machniewicz T. Numerical Modelling of Metal-Elastomer Spring Nonlinear Response for Low-Rate Deformations. Acta Mechanica et Automatica 2018; 12: 31–37.

31. Bowling S.R., Khasawneh M.T., Kaewkuekool S., Cho B.R. A Logistic Approximation to the Cumulative Normal Distribution. Journal of Industrial Engineering and Management 2009; 2: 114–127.

32. Hamasha M.M. Mathematical approximation of single- and double-sided truncated normal distribution using logistic function. International Journal of Industrial Engineering 2019; 26: 934–944, DOI:10.23055/ijietap.2019.26.6.3344.

33. Villanueva D., Feijóo A. Comparison of logistic functions for modeling wind turbine power curves. Electric Power Systems Research 2018; 155: 281–288, DOI:10.1016/j.epsr.2017.10.028.

34. Zhang L., Wu A., Wang H., Wang L. Representation of batch settling via fitting a logistic function. Minerals Engineering 2018; 128: 160–167, DOI:10.1016/j.mineng.2018.08.039.

35. Selech J., Andrzejczak K. Identification of Reliability Models for Non-repairable Railway Component. In: Kabashkin I., Yatskiv (Jackiva) I., Prentkovskis O. (eds) Reliability and Statistics in Transportation and Communication. RelStat 2018. Lecture Notes in Networks and Systems, vol 68. Springer, Cham: 2019, https://doi.org/10.1007/978-3-030-12450-2_49.

36. Świderski A., Jóźwiak A., Jachimowski R. Operational quality measures of vehicles applied for the transport services evaluation using artificial neural networks. Eksploatacja i Niezawodnosc – Maintenance and Reliability 2018; 20(2): 292–299, http://dx.doi.org/10.17531/ein.2018.2.16.